Electronic Supplementary Information

First application of Actinide Resin in the preparation of water samples for multi-actinide analysis with accelerator mass spectrometry

Thomas Roth,[a] Francesca Quinto,[a] Markus Plaschke,[a] Karin Hain, [b] Peter Steier,[b] Natalia Palina,[a] Sylvia Moisei-Rabung,[a] and Horst Geckeis[a]

[a] *Karlsruhe Institute of Technology (KIT), Institute for Nuclear Waste Disposal (INE), Hermann-von-Helmholtz-Platz 1, 76344 Eggenstein-Leopoldshafen, Germany. E-mail: thomas.roth@kit.edu*

[b] *University of Vienna, Faculty of Physics, Währinger Straße 17, 1090 Vienna, Austria.*

Contents

1 Isotopic composition of standard materials

Table S1 Isotopic composition of the standard material CBNM-IRM-040/1 that was used as ^{233}U spike solution. The uncertainty of the isotopic ratios is reported as "2 x standard deviation", as listed in the certificate

	Isotopic ratio
$^{234}U/^{233}U$	0.002373 ± 0.00014
$^{235}U/^{233}U$	0.000134 ± 0.00014
$^{236}U/^{233}U$	$< 0.0000015 \pm 0.0000017$
$^{238}U/^{233}U$	0.000485 ± 0.00014

	Proportion (at%)
^{233}U	99.7017
^{234}U	0.2366
^{235}U	0.0134
^{236}U	< 0.0002
^{238}U	0.0483

Table S2 Isotopic composition of the standard material CBNM IRM-042a that was used as ^{244}Pu spike solution. The uncertainty of the isotopic ratios is reported as "2 x standard deviation", as listed in the certificate

	Isotopic ratio
$^{238}Pu/^{244}Pu$	0.000055 ± 0.000007
$^{239}Pu/^{244}Pu$	0.000342 ± 0.000004
$^{240}Pu/^{244}Pu$	0.006918 ± 0.000012
$^{241}Pu/^{244}Pu$	0.000684 ± 0.000005
$^{242}Pu/^{244}Pu$	0.013611 ± 0.000010

	Proportion (at%)
^{238}Pu	0.0054
^{239}Pu	0.0335
^{240}Pu	0.6772
^{241}Pu	0.0670
^{242}Pu	1.3323
^{244}Pu	97.8846

2 Certified values and information values of CRM IAEA-381 and IAEA-443

2.1 IAEA-381

Table S3 Certified values of the CRM IAEA-381.[1] The uncertainty is reported as "1 x standard deviation". Values given in at/kg are calculated from the massic activities.

	Certified values (Bq/kg)	Certified values (at/kg)
^{237}Np	0.0087 ± 0.0005	(8.49 ± 0.49) x 10^{10}
^{238}Pu	0.0032 ± 0.0003	(1.28 ± 0.12) x 10^{6}
^{239}Pu	0.0081 ± 0.001	(8.89 ± 1.10) x 10^{8}
^{240}Pu	0.0066 ± 0.0004	(1.97 ± 0.12) x 10^{8}
^{241}Am	0.016 ± 0.003	(3.15 ± 0.59) x 10^{7}

Table S4 Information values of the CRM IAEA-381.[1] The uncertainty is reported as "1 x standard deviation". Values given in at/kg are calculated from the massic activities.

	Information values (Bq/kg)	Information values (at/kg)
^{234}U	0.051 ± 0.006	(5.70 ± 0.71) x 10^{10}
^{235}U	0.0021± 0.0004	(6.73 ± 1.28) x 10^{12}
^{236}U	0.0000192 ± 0.0000006	(2.05 ± 0.06) x 10^{9}
^{238}U	0.042 ± 0.004	(8.54 ± 0.81) x 10^{14}
^{241}Pu	0.23 ± 0.05	(1.50 ± 0.33) x 10^{7}
^{244}Cm	0.000032 ± 0.000009	(2.64 ± 0.74) x 10^{3}

2.2 IAEA-443

Table S5 Certified values of the CRM IAEA-443.[2] The uncertainty is reported as "1 x standard deviation". Values given in at/kg are calculated from the massic activities that are listed in the certificate.

	Certified values (Bq/kg)	Certified values (at/kg)
^{234}U	0.044 ± 0.002	(4.92 ± 0.22) x 10^{10}
^{235}U	0.00185 ± 0.0001	(5.93 ± 0.32) x 10^{12}
^{238}U	0.039 ± 0.002	(7.93 ± 0.41) x 10^{14}
^{238}Pu	0.0031 ± 0.0001	(1.24 ± 0.04) x 10^{6}
^{241}Am	0.0197 ± 0.001	(3.88 ± 0.20) x 10^{7}

Table S6 Information values of the CRM IAEA-443.[2] The uncertainty is reported as "1 x standard deviation". Values given in at/kg are calculated from the massic activities that are listed in the certificate.

	Information values (Bq/kg)	Information values (at/kg)
^{230}Th	0.5 ± 0.1	(1.72 ± 0.34) x 10^{8}
^{232}Th	0.19 ± 0.03	(1.22 ± 0.19) x 10^{13}
^{239}Pu	8.2 ± 0.8	(9.00 ± 0.88) x 10^{8}
^{240}Pu	7 ± 0.6	(2.09 ± 0.18) x 10^{8}
^{241}Pu	161 ± 19	(1.05 ± 0.12) x 10^{7}

3 RRW sampling information

Table S7 Sampling information and locations of the six Rhine River water (RRW) samples collected in the vicinity of the Fessenheim NPP

Sample ID	Location	Latitude	Longitude	Collection time
Grand Canal of Alsace:				
JR04	upstream	47° 50.64' N	7° 33.40' E	12.00 pm
JR10	at NPP	47° 54.40' N	7° 34.22' E	3.00 pm
JR08	downstream	47° 58.38' N	7° 36.70' E	4.00 pm
Old Rhine River:				
JR05	upstream	47° 50.65' N	7° 33.74' E	12.15 pm
JR11	at NPP	47° 54.49' N	7° 34.91' E	2.00 pm
JR09	downstream	47° 58.65' N	7° 37.37' E	11.00 pm

4 RRW separation efficiencies

Table S8 Separation efficiency (in per cent) of selected actinide and lanthanide elements of the RRW samples for separation via Actinide Resin or $Fe(OH)_3$ co-precipitation, determined by ICP-MS. Reported separation efficiencies are averages of six replicates. Reported uncertainties are 95% confidence intervals (n=6, k=2.571). A separation efficiency of 100 % would mean that all of the original sample content of the specific element was separated from the sample solution and would be found in the final AMS target material

	Separation efficiency (%)	
	RRW [Resin]	RRW [$Fe(OH)_3$]
^{238}U	80 ± 11	97 ± 3
^{232}Th	89 ± 9	97 ± 3
Ce	30 ± 14	99 ± 1
Gd	44 ± 21	95 ± 2

5 AMS analysis results of the individual RRW samples

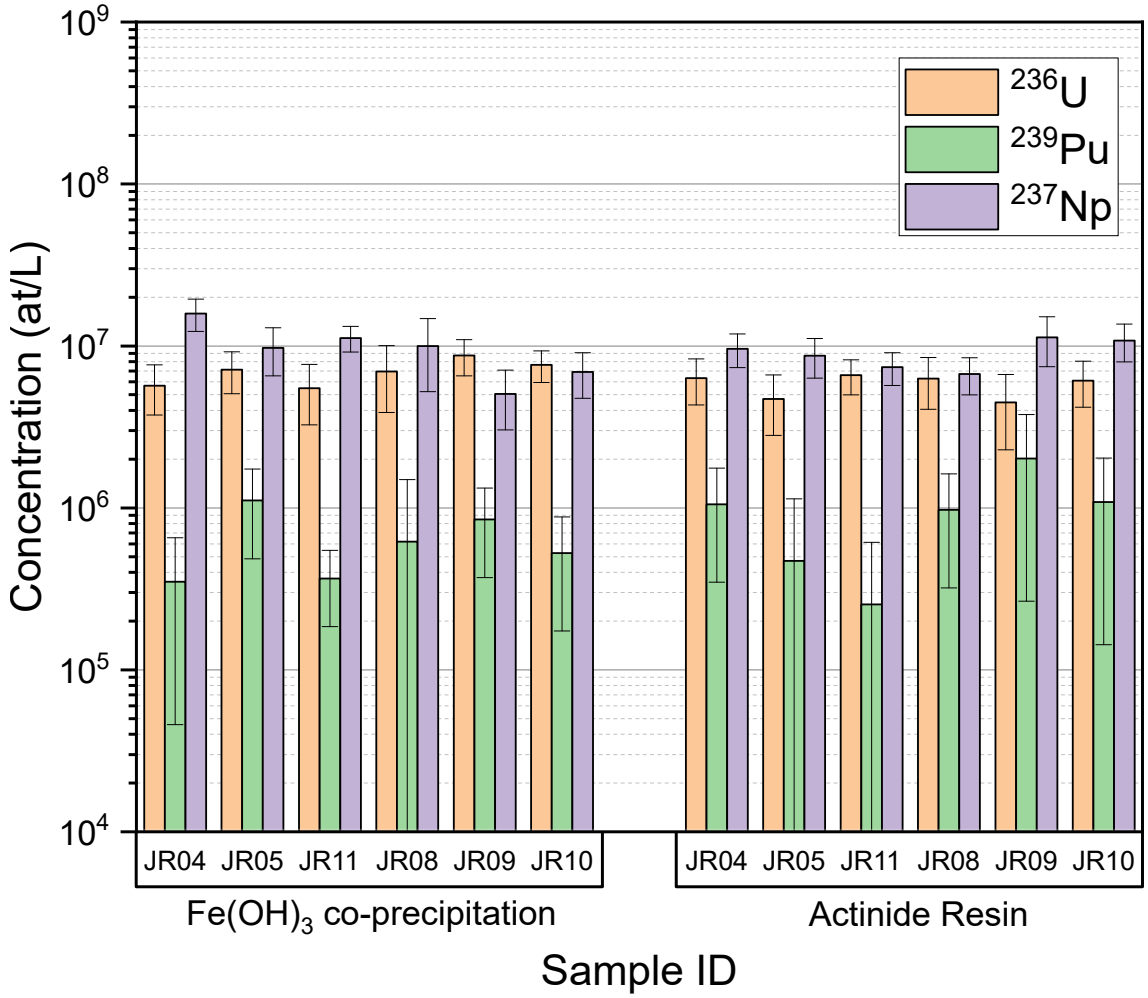

Figure S1 Results of the AMS analysis of individual Rhine River water (RRW) samples, sampled from different locations of the Rhine River, comparing both sample preparation methods. Error bars represent the propagated error from sample preparation and AMS analysis. The individual samples show no significant difference based on their sampling location. No influence of the Fessenheim NPP on the actinide content of the river water could be detected.

6 Actinide Resin uptake for varying sorption times

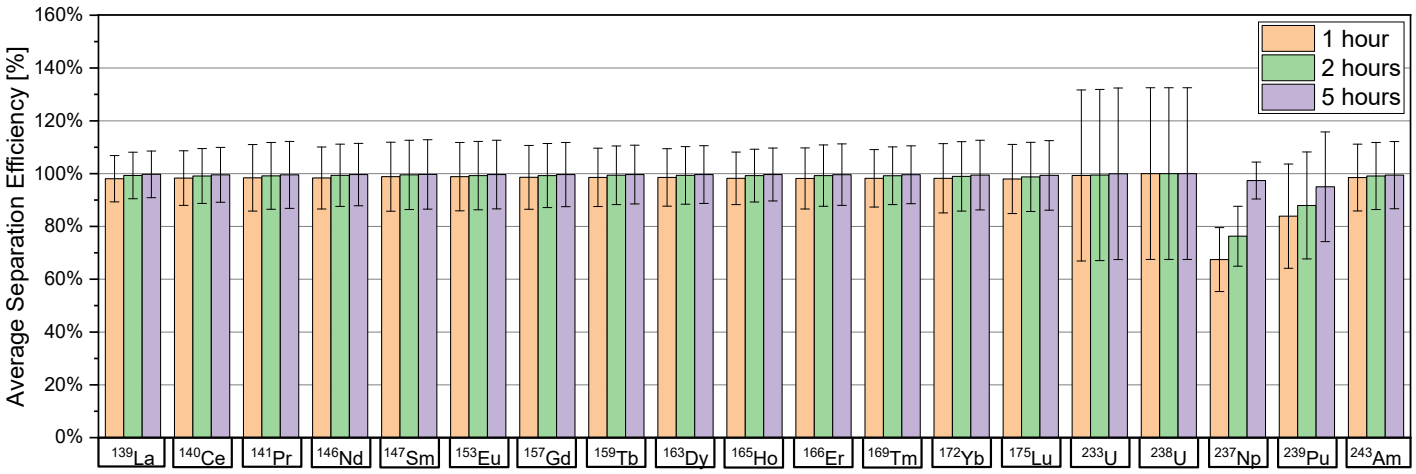

Figure S2 Uptake experiment for Actinide Resin with varying sorption times. Reported separation efficiencies are averages of three replicates. Error bars represent 95% confidence intervals (n=3, k=4.303). 10 mL solutions of 5 ng/L ^{233}U, ^{237}Np, ^{239}Pu, ^{243}Am, ^{248}Cm and 5µg/L ^{232}Th, ^{238}U, Lanthanides were contacted with 2.5 mg Actinide Resin in a stirred batch reaction with sorption times of 1 h, 2 h or 5 h. Concentrations were chosen to be appropriate for analysis with SF-ICP-MS. ^{237}Np and ^{239}Pu uptake was near quantitative only for sorption times of 5 h. A separation efficiency of 100% indicates that 100% of the respective nuclide was separated from the solution and is sorbed on Actinide Resin.

7 Dataset of AMS analysis concentration graphs in main article

Table S9 Dataset of concentration bar graph depicted in Figure 2 in the main article

	Concentration (at/L)	95% CI (at/L)
^{236}U		
Actinide Resin	5.8×10^{6}	1.0×10^{6}
$Fe(OH)_3$ co-precipitation	6.9×10^{6}	1.3×10^{6}
^{239}Pu		
Actinide Resin	9.8×10^{5}	6.4×10^{5}
$Fe(OH)_3$ co-precipitation	6.4×10^{5}	3.1×10^{5}
^{237}Np		
Actinide Resin	9.1×10^{6}	1.9×10^{6}
$Fe(OH)_3$ co-precipitation	9.8×10^{6}	3.9×10^{6}

Table S10 Dataset of concentration bar graph depicted in Figure 3 in the main article

	Concentration (at/L)	Propagated error (at/L)
^{236}U		
Actinide Resin	1.7×10^{9}	2×10^{8}
	1.3×10^{9}	2×10^{8}
$Fe(OH)_3$ co-precipitation	1.8×10^{9}	1×10^{8}
	1.7×10^{9}	1×10^{8}
^{239}Pu		
Actinide Resin	9.2×10^{8}	6×10^{7}
	7.4×10^{8}	5×10^{7}
$Fe(OH)_3$ co-precipitation	8.6×10^{8}	6×10^{7}
	7.6×10^{8}	6×10^{7}
^{240}Pu		
Actinide Resin	1.9×10^{8}	1×10^{7}
	1.8×10^{8}	1×10^{7}
$Fe(OH)_3$ co-precipitation	1.9×10^{8}	1×10^{7}
	1.9×10^{8}	2×10^{7}
^{237}Np		
Actinide Resin	9.3×10^{10}	1.0×10^{10}
	5.9×10^{10}	1.0×10^{10}
	8.0×10^{10}	8×10^{9}
$Fe(OH)_3$ co-precipitation	1.1×10^{11}	1×10^{10}
	1.5×10^{11}	1×10^{10}
	1.18×10^{11}	7×10^{9}

8 ICP-OES results

8.1 RRW sample system

Table S11 RRW sample system (2 L aliquots). Sample content of common matrix elements determined via ICP-OES before and after separation of the analytes from solution with Actinide Resin. The sample content is reported for replicate samples. Reported uncertainties represent the propagated error from sample preparation and ICP-OES analysis. Before separation: analysis of RRW sample aliquot; after separation: analysis of eluent after batch sorption on Actinide Resin. The sample content after separation represents the sample matrix that was not separated with Actinide Resin and, thus, will not be found in the final AMS target material

	Sample content (mg/sample)				Sample content (μg/sample)					
	Ca	Na	Mg	K	Si	Sr	Al	Fe	Mn	Ba
Before:										
JR05	65.5 ± 0.9	18.5 ± 0.4	14.3 ± 0.1	3.57 ± 0.04	66.5 ± 4.2	714 ± 12	492 ± 7	224 ± 3	21.0 ± 1.1	27.4 ± 0.7
JR11	63.7 ± 1.8	15.1 ± 0.2	14.2 ± 0.2	3.19 ± 0.06	80.2 ± 5.7	716 ± 10	322 ± 8	162 ± 3	14.4 ± 0.3	26.1 ± 0.3
JR09	63.4 ± 0.9	18.2 ± 0.4	14.6 ± 0.2	3.63 ± 0.09	89.7 ± 4.4	719 ± 14	472 ± 15	219 ± 6	16.2 ± 0.4	28.4 ± 0.4
After:										
JR05	101.6 ± 1.2	17.8 ± 0.4	13.8 ± 0.3	3.52 ± 0.04	83.3 ± 5.6	722 ± 7	479 ± 8	158 ± 3	18.4 ± 0.9	28.8 ± 0.6
JR11	99.0 ± 2.8	14.3 ± 0.2	13.3 ± 0.2	3.07 ± 0.06	88.1 ± 4.8	698 ± 8	302 ± 4	122 ± 1	12.8 ± 0.2	24.5 ± 0.3
JR09	102.1 ± 1.1	18.2 ± 0.4	14.3 ± 0.2	3.50 ± 0.04	100.4 ± 4.7	737 ± 9	463 ± 9	156 ± 2	15.9 ± 0.4	27.9 ± 0.5

Table S12 RRW sample system (2 L aliquots). Sample content of common matrix elements determined via ICP-OES before and after separation of the analytes from solution via $Fe(OH)_3$ co-precipitation. The sample content is reported for replicate samples. Reported uncertainties represent the propagated error from sample preparation and ICP-OES analysis. Before separation: analysis of RRW sample aliquot; after separation: analysis of supernatant after $Fe(OH)_3$ co-precipitation. The sample content after separation represents the sample matrix that was not separated via $Fe(OH)_3$ co-precipitation and, thus, will not be found in the final AMS target material

	Sample content (mg/sample)				Sample content (μg/sample)					
	Ca	Na	Mg	K	Si	Sr	Al	Fe	Mn	Ba
Before:										
JR05	107 ± 1	17.8 ± 0.4	15.1 ± 0.2	3.59 ± 0.04	780 ± 9	731 ± 18	427 ± 6	198 ± 3	16.1 ± 0.3	82.8 ± 1.2
JR11	104 ± 2	14.6 ± 0.4	14.2 ± 0.4	3.27 ± 0.06	814 ± 20	723 ± 11	315 ± 8	128 ± 3	12.7 ± 0.3	69.3 ± 0.9
JR09	104 ± 1	17.8 ± 0.7	14.8 ± 0.3	3.61 ± 0.09	805 ± 9	717 ± 9	394 ± 5	196 ± 3	16.0 ± 0.2	82.1 ± 1.8
After:										
JR05	167 ± 2	17.6 ± 0.4	14.9 ± 0.2	3.54 ± 0.06	135 ± 2	718 ± 18	47.9 ± 3.1	25.1 ± 0.5	10.7 ± 0.1	77.7 ± 0.9
JR11	165 ± 2	14.7 ± 0.4	14.6 ± 0.2	3.23 ± 0.08	153 ± 2	739 ± 20	46.3 ± 1.0	18.7 ± 0.4	9.5 ± 0.1	65.7 ± 1.1
JR09	170 ± 4	18.0 ± 0.4	14.8 ± 0.3	3.47 ± 0.06	100 ± 2	721 ± 8	56.5 ± 2.3	17.1 ± 0.3	10.9 ± 0.1	77.5 ± 0.9

8.2 CRM sample system

Table S13 CRM sample system (100 mL aliquots; 1st AMS analysis). Sample content of common matrix elements determined via ICP-OES before and after separation of the analytes from solution via $Fe(OH)_3$ co-precipitation. The sample content is reported for replicate samples. Reported uncertainties represent the propagated error from sample preparation and ICP-MS analysis. Before separation: analysis of CRM sample aliquot; after separation: analysis of supernatant after $Fe(OH)_3$ co-precipitation. The sample content after separation represents the sample matrix that was not separated via $Fe(OH)_3$ co-precipitation and, thus, will not be found in the final AMS target material

	Sample content (mg/sample)						Sample content (μg/sample)			
	Ca	Na	Mg	K	Al	Fe	Si	Sr	Mn	Ba
Before:										
C1	40.7 ± 0.5	1027 ± 15	38.8 ± 0.6	3.52 ± 0.05	1.09 ± 0.02	1.15 ± 0.02	102 ± 2	824 ± 11	15.8 ± 1.0	906 ± 60
C2	41.0 ± 0.5	1069 ± 20	38.9 ± 0.4	3.27 ± 0.05	1.09 ± 0.05	1.16 ± 0.02	105 ± 2	826 ± 10	0.327 ± 0.005	891 ± 86
After:										
C1	41.4 ± 0.5	1058 ± 34	41.5 ± 0.6	4.21 ± 0.06	1.16 ± 0.04	0.00 ± 0.00	91 ± 1	820 ± 12	0.421 ± 0.006	857 ± 69
C2	39.7 ± 0.5	1031 ± 13	42.4 ± 1.2	3.90 ± 0.05	1.17 ± 0.02	0.04 ± 0.01	100 ± 1	822 ± 12	0.390 ± 0.005	863 ± 383

Table S14 CRM sample system (100 mL aliquots; 1st AMS analysis). Sample content of common matrix elements determined via ICP-OES before and after separation of the analytes from solution via Actinide Resin. The sample content is reported for replicate samples. Reported uncertainties represent the propagated error from sample preparation and ICP-MS analysis. Before separation: analysis of CRM sample aliquot; after separation: analysis of eluent after batch sorption on Actinide Resin. The sample content after separation represents the sample matrix that was not separated with Actinide Resin and, thus, will not be found in the final AMS target material

	Sample content (mg/sample)						Sample content (μg/sample)			
	Ca	Na	Mg	K	Al	Fe	Si	Sr	Mn	Ba
Before:										
R1	40.6 ± 0.5	1059 ± 18	38.1 ± 1.0	2.61 ± 0.04	1.28 ± 0.04	1.19 ± 0.02	108 ± 1	824 ± 9	0.261 ± 0.004	906 ± 68
R2	41.1 ± 0.5	1026 ± 19	37.9 ± 0.5	2.33 ± 0.03	1.21 ± 0.02	1.18 ± 0.02	107 ± 2	831 ± 12	0.233 ± 0.003	899 ± 52
After:										
R1	40.3 ± 0.5	1025 ± 21	42.2 ± 0.7	3.25 ± 0.05	1.11 ± 0.03	0.93 ± 0.01	103 ± 2	825 ± 10	0.325 ± 0.005	895 ± 53
R2	40.6 ± 0.9	1045 ± 39	40.7 ± 0.5	2.97 ± 0.04	1.08 ± 0.03	0.96 ± 0.01	104 ± 2	808 ± 10	0.297 ± 0.004	887 ± 149

9 Artificial sea water (ASTM D1141-98)

Table S15 Composition of the artificial sea water used to simulate sea water matrix. Prepared with "Sea Salt" ASTM D1141-98, containing all elements found in natural sea water in quantities greater than 0.0004 wt%. Left: Solid sea salt composition as percentage of total weight according to label. Right: Calculated component concentration of 100 mL artificial sea water aliquot

	Composition (wt%)
NaCl	58.490
$MgCl_2 \cdot 6H_2O$	26.460
Na_2SO_4	9.750
$CaCl_2$	2.765
KCl	1.645
$NaHCO_3$	0.477
KBr	0.238
$SrCl_2 \cdot 6H_2O$	0.095
H_3BO_3	0.071
NaF	0.007

	Concentration (mg/100mL)
Cl^-	1983.8
Na^+	1042.6
SO_4^{2-}	276.6
Mg^{2+}	132.7
Ca^{2+}	41.9
K^+	39.5
CO_3^{2-}	14.3
Br^-	6.7
BO_3^{3-}	2.8
Sr^{2+}	1.3
F^-	0.1

10 SEM-EDS results

All target materials were measured with AMS, before the SEM-EDS analysis. The Al sample holders were sputtered with Cs throughout the AMS measurement, resulting in visible degradation. For SEM-EDS analysis, the residual target material was scraped out of the sample holder, pressed onto In foil and coated with C to prevent a fast charge-up of the surface. As such, the EDS signals for Al, Cs, In or C in the target materials could not be assigned as original content of the materials and those elements are assumed to have been introduced throughout the AMS measurement or the SEM-EDS sample preparation.

10.1 RRW target materials

10.1.1 RRW sample JR05

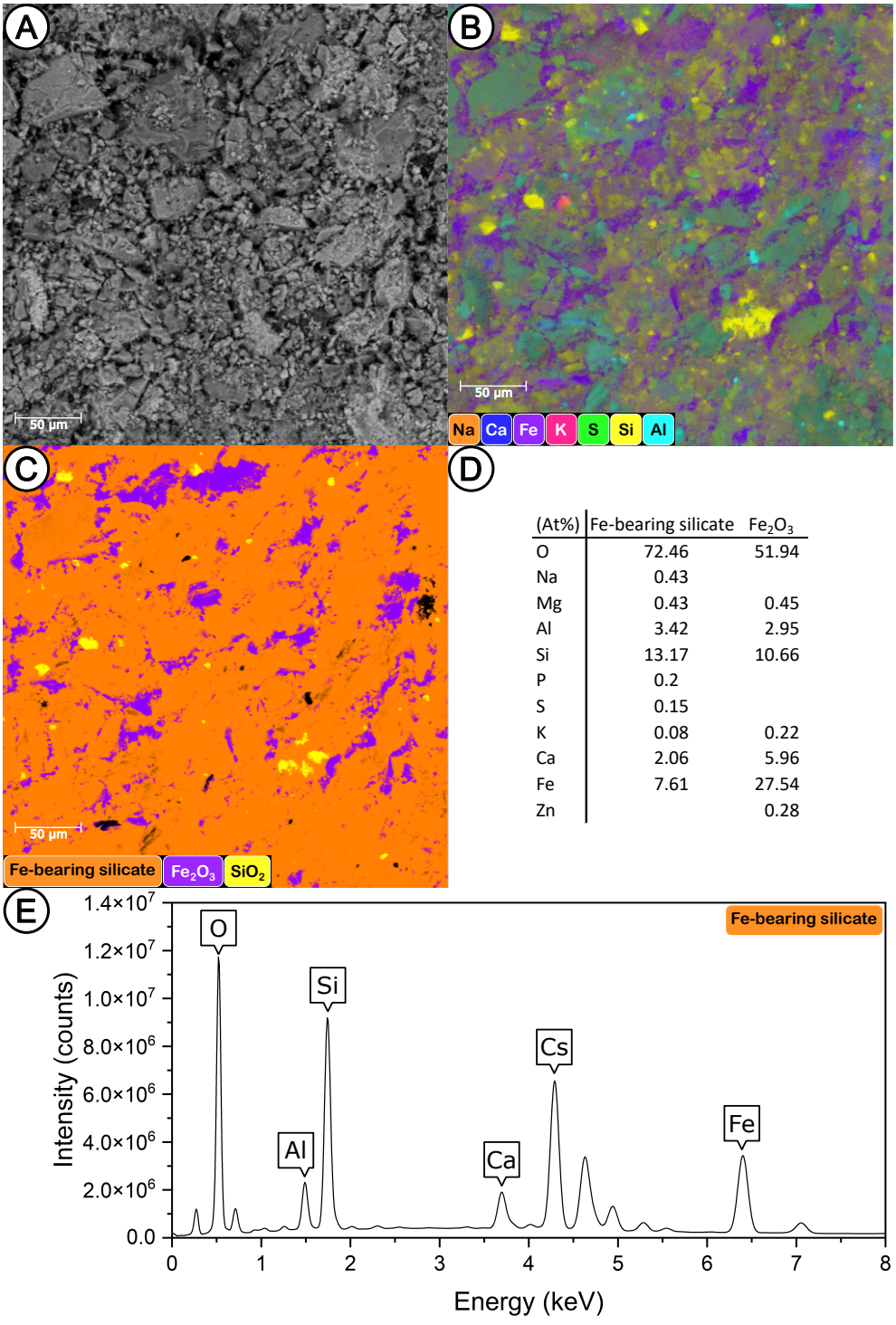

Figure S3 SEM-EDS results for AMS target material of RRW sample JR05; prepared by $Fe(OH)_3$ co-precipitation. (A) SEM image of the sample material, recorded with a backscattered electron (BSE) detector (B) Elemental EDS map, depicting the most abundant element. (C) Phase EDS map, depicting regions of similar elemental composition. (D) EDS results for the two most abundant phases; a relative error of ± 2–5 % is expected for major components, whereas a relative error as high as ± 30–50 % is expected for minor components and light elements. (E) EDS spectrum of the most abundant phase.

Figure S3 shows the results of the SEM-EDS analysis of the target material of RRW sample JR05, which was prepared by $Fe(OH)_3$ co-precipitation. No significant difference was detected for the six individual RRW samples (Figure S1). As such, they are assumed to be replicates, and sample JR05 should be representative of all of the RRW samples. The target material is composed of three major phases, distinct phases of SiO_2 and Fe_2O_3, as well as an in-between phase that is either a mixture of SiO_2 and Fe_2O_3 or Fe-bearing silicate. This confirms that silicate is the major sample matrix and the source of the observed increased mass (multiple times the intended mass) of the final AMS target material for the RRW samples prepared by $Fe(OH)_3$ co-precipitation. The silicate content was present in the RRW as undigested particulate matter, which was transferred together with the co-precipitated $Fe(OH)_3$, and potentially dissolved Si that was precipitated concurrently with the $Fe(OH)_3$ co-precipitation.

10.1.2 RRW procedure blank

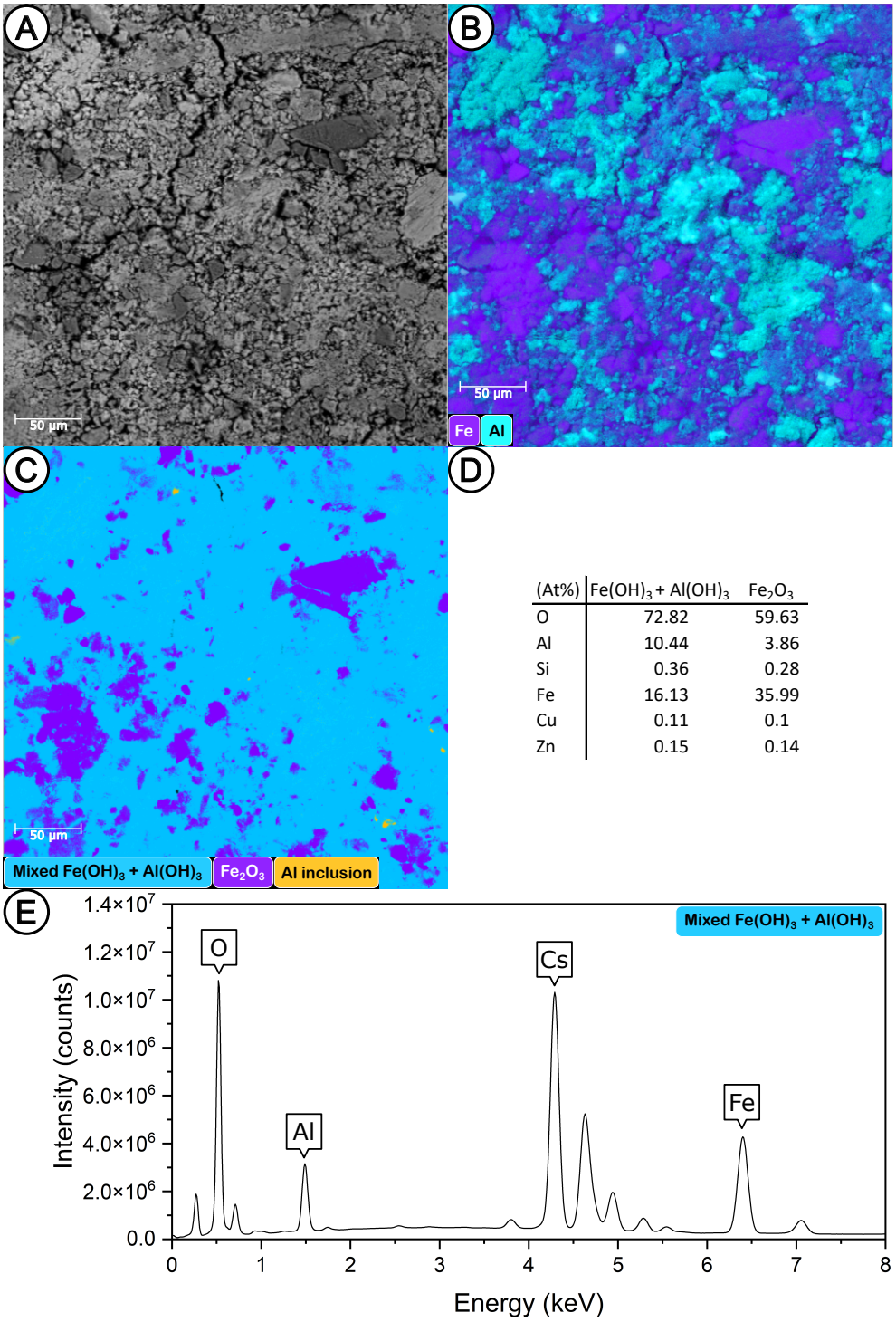

(At%)	$Fe(OH)_3 + Al(OH)_3$	Fe_2O_3
O	72.82	59.63
Al	10.44	3.86
Si	0.36	0.28
Fe	16.13	35.99
Cu	0.11	0.1
Zn	0.15	0.14

Figure S4 SEM-EDS results for AMS target material of RRW procedure blank. (A) SEM image of the sample material, recorded with a backscattered electron (BSE) detector (B) Elemental EDS map, depicting the most abundant element. (C) Phase EDS map, depicting regions of similar elemental composition. (D) EDS results for the two most abundant phases; a relative error of ± 2–5 % is expected for major components, whereas a relative error as high as ± 30–50 % is expected for minor components and light elements. (E) EDS spectrum of the most abundant phase.

Figure S4 shows the results of the SEM-EDS analysis of the target material of a RRW procedure blank, which was prepared by $Fe(OH)_3$ co-precipitation identically to the RRW samples, without addition of any synthetic matrix. This blank target material, therefore, represents an AMS sample prepared by $Fe(OH)_3$ co-precipitation that is free of sample matrix. The phase EDS map shows two major phases, distinct Fe_2O_3 and what is likely a mixture of $Fe(OH)_3$ and $Al(OH)_3$. The high Al content originates from the degradation of the Al target throughout the sputtering in the AMS ion source, while the uncommon phase of elemental Al likely stems from the Al target, of which the target material was scraped out manually, resulting in Al particles.

10.2 CRM target materials (1st AMS analysis)

10.2.1 CRM sample prepared by $Fe(OH)_3$ co-precipitation

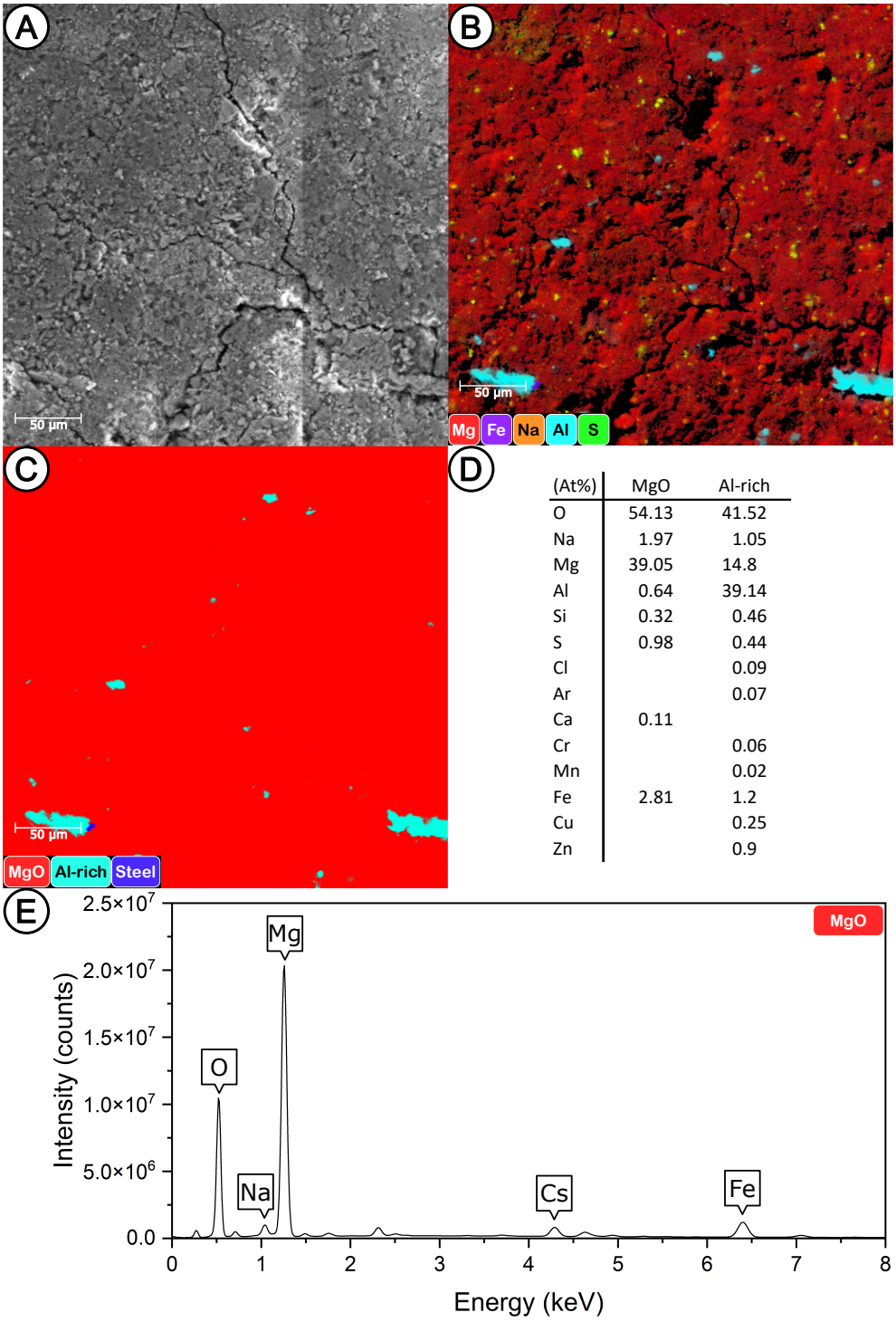

(At%)	MgO	Al-rich
O	54.13	41.52
Na	1.97	1.05
Mg	39.05	14.8
Al	0.64	39.14
Si	0.32	0.46
S	0.98	0.44
Cl		0.09
Ar		0.07
Ca	0.11	
Cr		0.06
Mn		0.02
Fe	2.81	1.2
Cu		0.25
Zn		0.9

Figure S5 SEM-EDS results for AMS target material of a CRM sample of the 1st AMS analysis; prepared by $Fe(OH)_3$ co-precipitation. (A) SEM image of the sample material, recorded with a backscattered electron (BSE) detector (B) Elemental EDS map, depicting the most abundant element. (C) Phase EDS map, depicting regions of similar elemental composition. (D) EDS results for the two most abundant phases; a relative error of ± 2–5 % is expected for major components, whereas a relative error as high as ± 30–50 % is expected for minor components and light elements. (E) EDS spectrum of the most abundant phase.

Figure S5 shows the results of the SEM-EDS analysis of the target material of a CRM sample from the 1st AMS analysis, which was prepared by $Fe(OH)_3$ co-precipitation. The phase EDS map shows a major phase of MgO, which has likely precipitated as $Mg(OH)_2$ concurrently with the $Fe(OH)_3$ co-precipitation. Mg is one of the most abundant components of sea water. This implies that the significant matrix mass that was present in the CRM samples of the 1st AMS analysis was MgO, resulting in a dilution effect and low count rates in the AMS analysis. The less abundant Al-rich phase and the minor steel phase likely originate from degradation of the Al sample holder and from abrasion of the steel tool that was used to scrape the target material out of the target, respectively.

10.2.2 CRM sample prepared by Actinide Resin

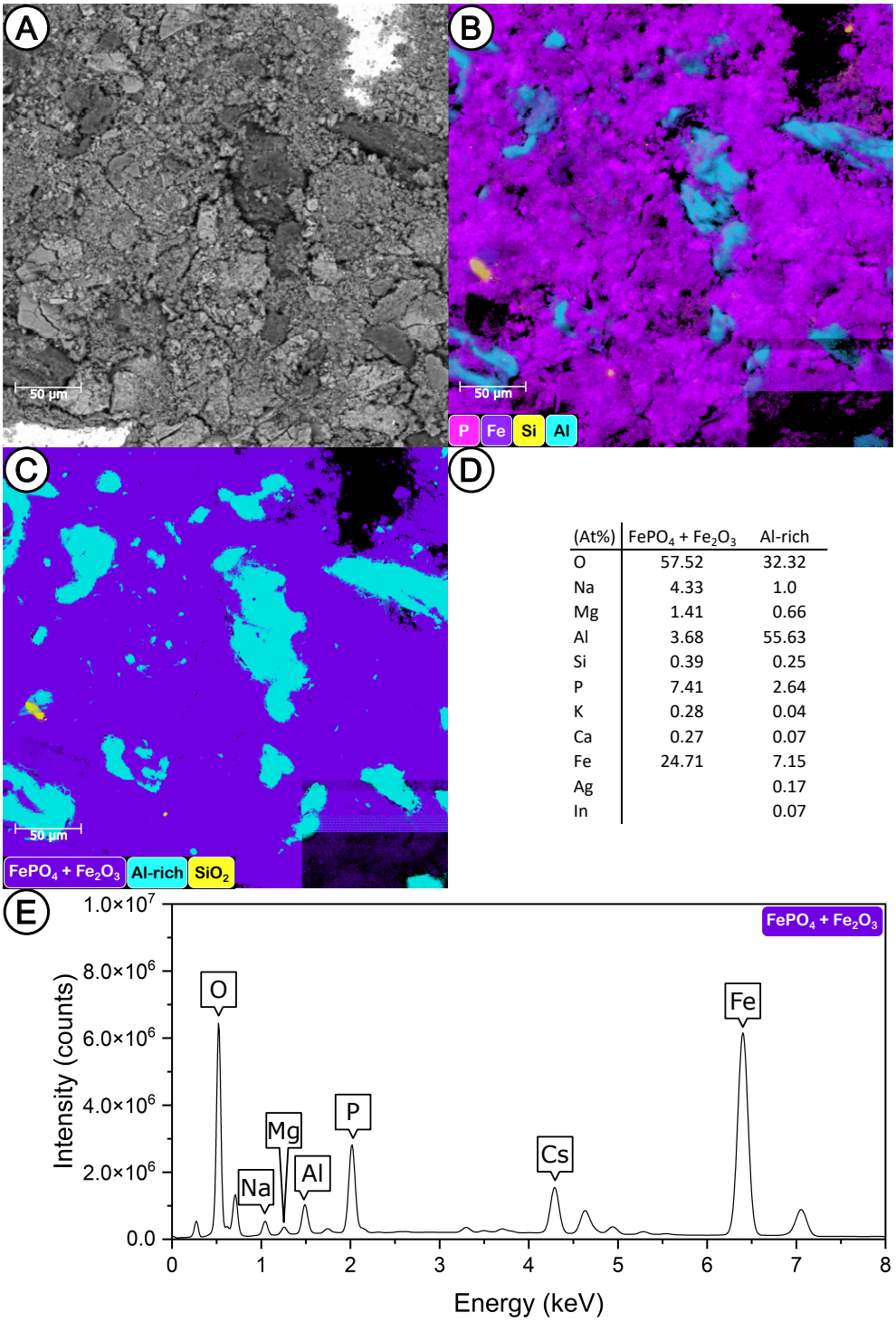

(At%)	$FePO_4 + Fe_2O_3$	Al-rich
O	57.52	32.32
Na	4.33	1.0
Mg	1.41	0.66
Al	3.68	55.63
Si	0.39	0.25
P	7.41	2.64
K	0.28	0.04
Ca	0.27	0.07
Fe	24.71	7.15
Ag		0.17
In		0.07

Figure S6 SEM-EDS results for AMS target material of a CRM sample of the 1st AMS analysis; prepared by Actinide Resin. (A) SEM image of the sample material, recorded with a backscattered electron (BSE) detector (B) Elemental EDS map, depicting the most abundant element. (C) Phase EDS map, depicting regions of similar elemental composition. (D) EDS results for the two most abundant phases; a relative error of ± 2–5 % is expected for major components, whereas a relative error as high as ± 30–50 % is expected for minor components and light elements. (E) EDS spectrum of the most abundant phase. The black box and lines in the bottom right of (B) and (C) are analytical artefacts.

Figure S6 shows the results of the SEM-EDS analysis of the target material of a CRM sample from the 1st AMS analysis, which was prepared by Actinide Resin. The phase EDS map shows a major phase that is likely a mixture of $FePO_4$ and Fe_2O_3. The functional group of the DIPEX® extractant of Actinide Resin, which is responsible for bonding with the actinide analytes, is a diphosphonic acid. Decomposition of the extractant can yield phosphoric acid,[3] which is presumably the source of the phosphate. The less abundant Al-rich phase likely originates from degradation of the Al sample holder.

10.3 CRM target materials (2nd AMS analysis)

10.3.1 CRM sample prepared by $Fe(OH)_3$ co-precipitation

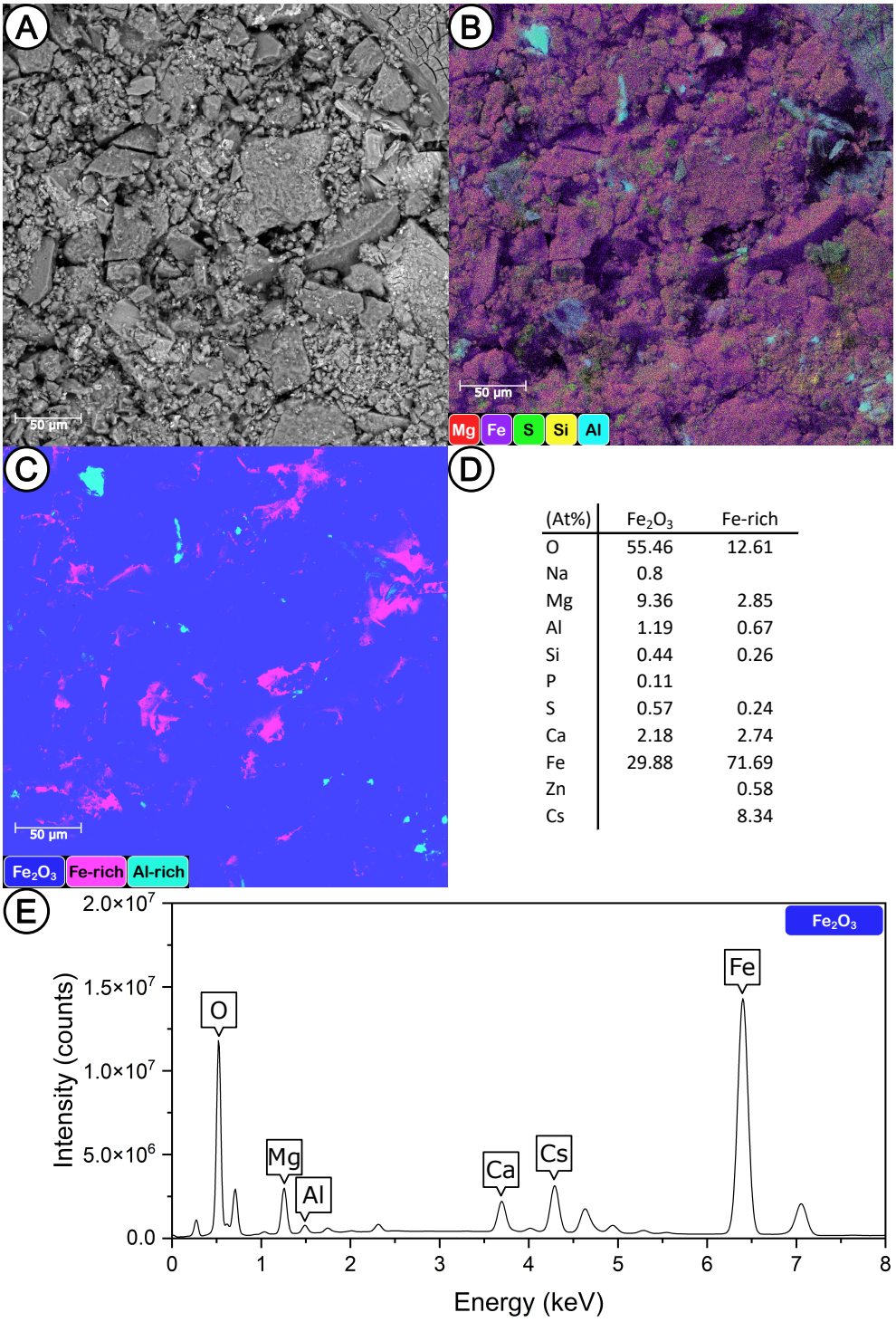

(At%)	Fe_2O_3	Fe-rich
O	55.46	12.61
Na	0.8	
Mg	9.36	2.85
Al	1.19	0.67
Si	0.44	0.26
P	0.11	
S	0.57	0.24
Ca	2.18	2.74
Fe	29.88	71.69
Zn		0.58
Cs		8.34

Figure S7 SEM-EDS results for AMS target material of a CRM sample of the 2nd AMS analysis; prepared by $Fe(OH)_3$ co-precipitation. (A) SEM image of the sample material, recorded with a backscattered electron (BSE) detector (B) Elemental EDS map, depicting the most abundant element. (C) Phase EDS map, depicting regions of similar elemental composition. (D) EDS results for the two most abundant phases; a relative error of ± 2–5 % is expected for major components, whereas a relative error as high as ± 30–50 % is expected for minor components and light elements. (E) EDS spectrum of the most abundant phase.

Figure S7 shows the results of the SEM-EDS analysis of the target material of a CRM sample from the 2nd AMS analysis, which was prepared by $Fe(OH)_3$ co-precipitation. The phase EDS map shows a major phase of Fe_2O_3, containing a minor amount of Mg, likely in the form of MgO. In contrast to the CRM sample of the 1st AMS analysis that was also prepared by $Fe(OH)_3$ co-precipitation (Figure S5), only a minor amount of matrix was precipitated, resulting in lower total mass of the target material, a reduced dilution effect and higher count rates in the AMS analysis. The less abundant Fe-rich phase with > 70 at% Fe indicates the presence of metallic Fe, while the minor Al-rich phase likely originates from degradation of the Al sample holder.

10.3.2 CRM sample prepared by Actinide Resin

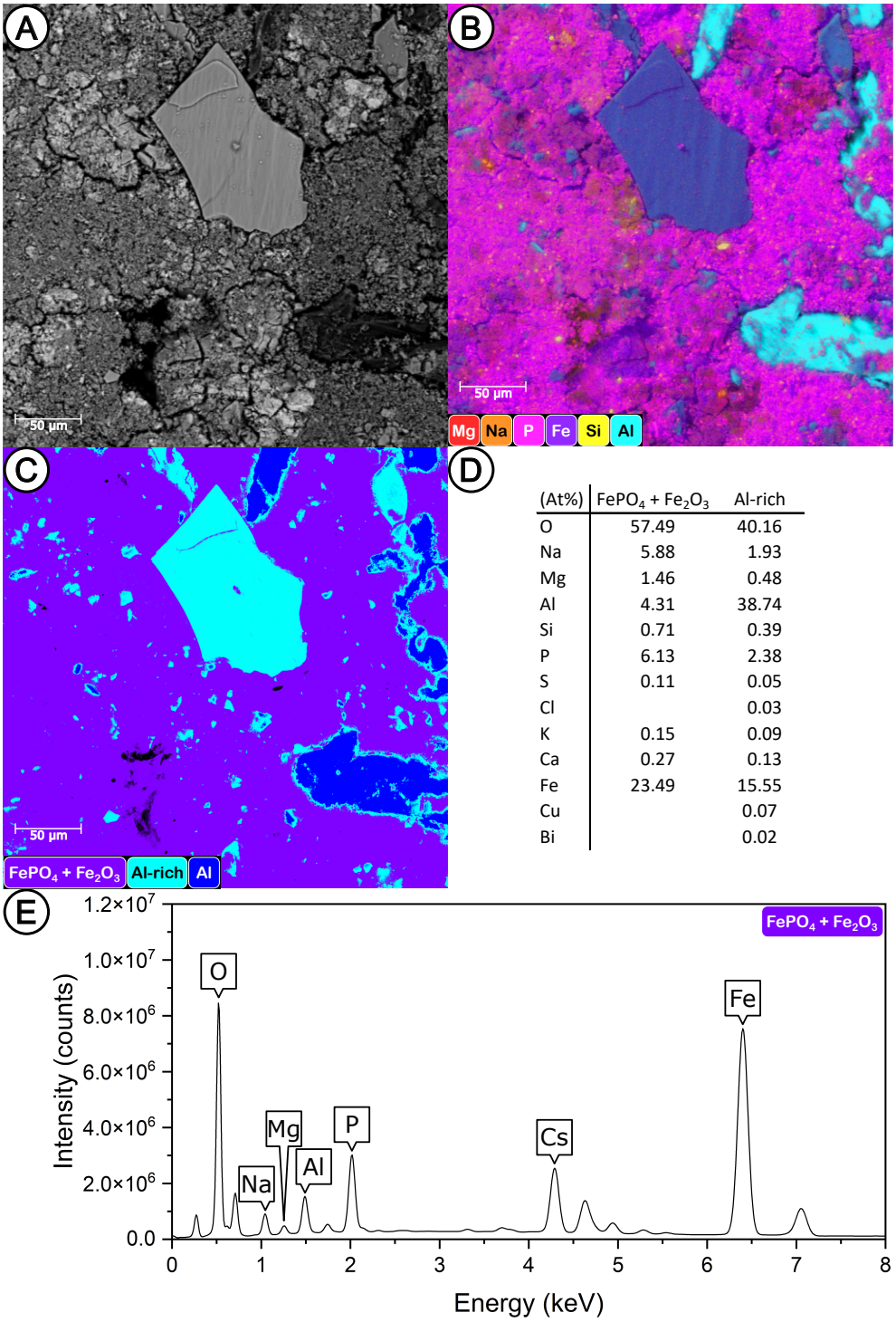

(At%)	$FePO_4 + Fe_2O_3$	Al-rich
O	57.49	40.16
Na	5.88	1.93
Mg	1.46	0.48
Al	4.31	38.74
Si	0.71	0.39
P	6.13	2.38
S	0.11	0.05
Cl		0.03
K	0.15	0.09
Ca	0.27	0.13
Fe	23.49	15.55
Cu		0.07
Bi		0.02

Figure S8 SEM-EDS results for AMS target material of a CRM sample of the 2nd AMS analysis; prepared by Actinide Resin. (A) SEM image of the sample material, recorded with a backscattered electron (BSE) detector (B) Elemental EDS map, depicting the most abundant element. (C) Phase EDS map, depicting regions of similar elemental composition. (D) EDS results for the two most abundant phases; a relative error of ± 2–5 % is expected for major components, whereas a relative error as high as ± 30–50 % is expected for minor components and light elements. (E) EDS spectrum of the most abundant phase.

Figure S8 shows the results of the SEM-EDS analysis of the target material of a CRM sample from the 2nd AMS analysis, which was prepared by Actinide Resin. The phase EDS map shows a major phase that is likely a mixture of $FePO_4$ and Fe_2O_3. The functional group of the DIPEX® extractant of Actinide Resin, which is responsible for bonding with the actinide analytes, is a diphosphonic acid. Decomposition of the extractant can yield phosphoric acid,[3] which is presumably the source of the phosphate. The less abundant Al-rich phase and metallic Al phase likely originate from degradation of the Al sample holder, as well as abrasion when the target material was scraped out of the Al sample holder, respectively.

11 SEM-EDS / PXRD

11.1 Identification of RRW sample matrix precipitate

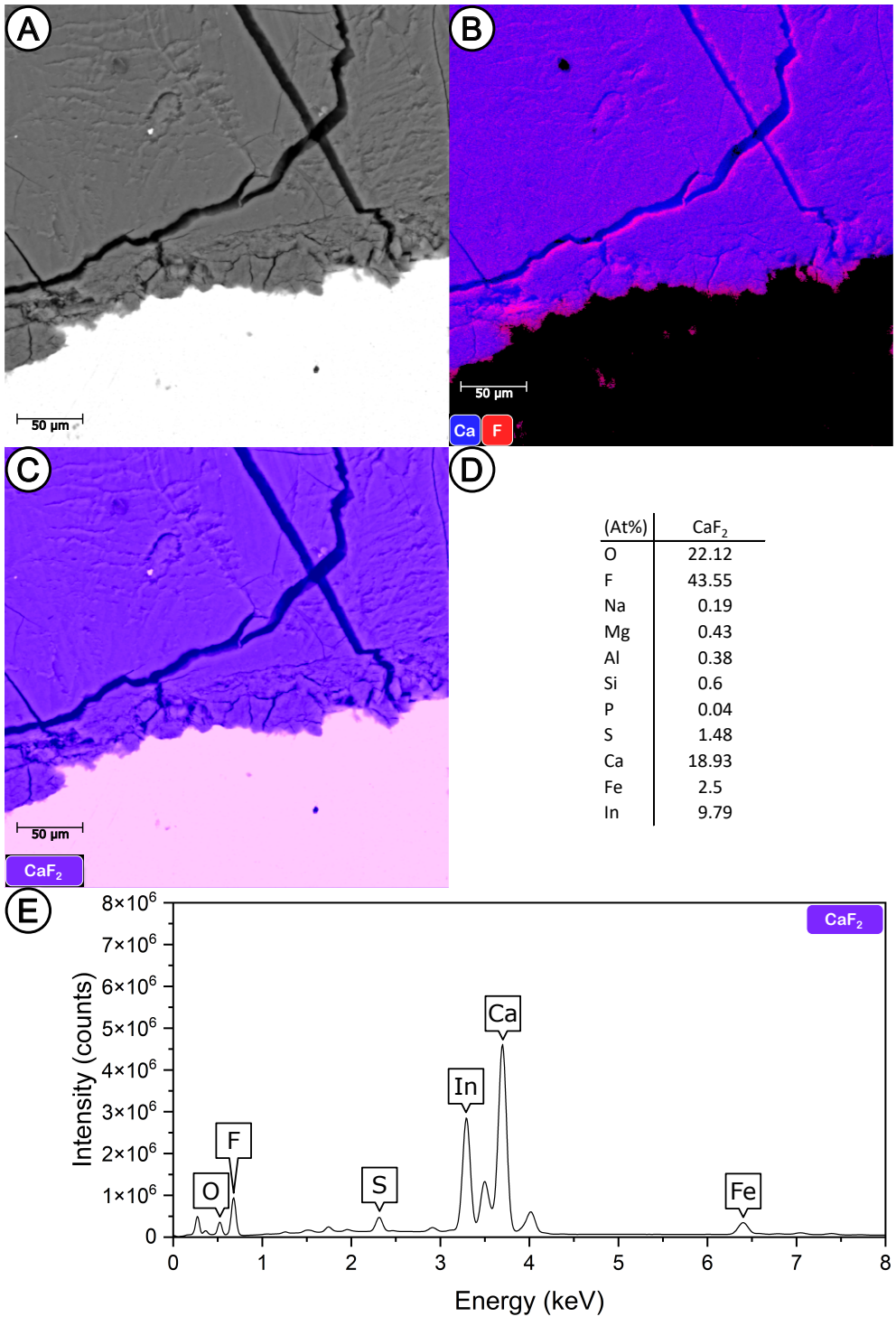

Figure S9 SEM-EDS results for $Fe(OH)_3$ co-precipitate from supernatant of RRW sample after batch reaction with Actinide Resin. (A) SEM image of the sample material, recorded with a backscattered electron (BSE) detector (B) Elemental EDS map, depicting the most abundant element. (C) Phase EDS map, depicting regions of similar elemental composition. (D) EDS results for the detected phase; a relative error of ± 2–5 % is expected for major components, whereas a relative error as high as ± 30–50 % is expected for minor components and light elements. (E) EDS spectrum of the detected phase.

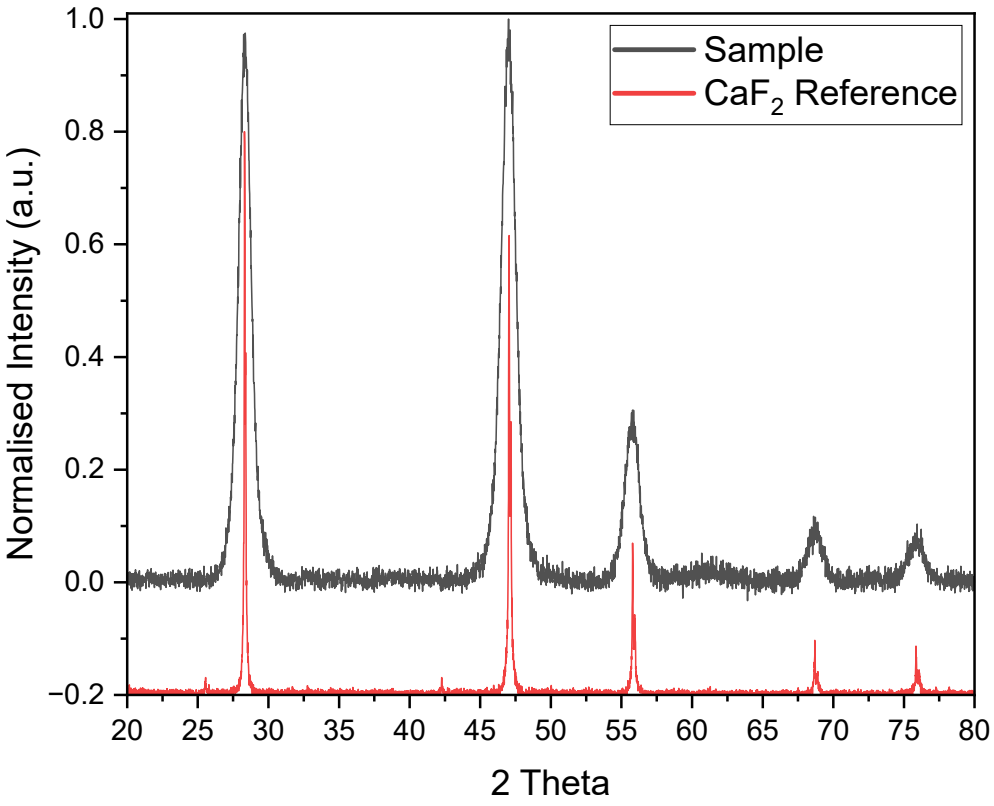

Figure S10 X-ray Powder Diffraction (XRPD) analysis of RRW sample. Precipitated with $Fe(OH)_3$ co-precipitation from supernatant solution after batch reaction with Actinide Resin. The CaF_2 reference data originates from the RRUFF Project database.[4]

As stated in the article (Section 2.4.1), $Fe(OH)_3$ co-precipitation from the RRW samples in which all particulate matter was digested with a mixture of HF and HNO_3 resulted in precipitation of sample matrix in such large quantities that the sample preparation could not be continued. Subsequently, the precipitate was redissolved and Actinide Resin was used for sample preparation. To investigate the composition of this sample matrix precipitate, an $Fe(OH)_3$ co-precipitation was carried out from the supernatant solution after batch reaction with Actinide Resin and filtration of the resin, again resulting in precipitation of large quantities of sample matrix. Assuming that only insignificant amounts of sample matrix were removed from solution with Actinide Resin, this precipitate should be near identical to the one of the first $Fe(OH)_3$ co-precipitation attempt that was redissolved.

The results of a SEM-EDS analysis of this sample matrix precipitate are depicted in Figure S9. The phase EDS map shows only a single homogeneous phase, of which CaF_2 seems to be the major component. Because of addition of significant amounts of boric acid to mask the fluoride content after digestion with HF and prevent precipitation of fluorides, the matrix precipitate could also have been a salt containing boron, e.g. $Ca(BF_4)_2$. Since SEM-EDS cannot detect boron, as its emitted photons are too low energy to pass the entrance window of the EDS detector, the precipitate was further analysed with X-ray Powder Diffraction (XRPD). As can be seen in Figure S10, the sample diffractogram is in good agreement with a CaF_2 reference diffractogram.[4]

12 Further comments on practical application of Actinide Resin for multi-actinide AMS sample preparation

There are some practical considerations for the use of Actinide Resin for AMS sample preparation that are noteworthy for a successful application of the method.

AMS analysis is generally performed with low masses of target material. For an $Fe(OH)_3$ co-precipitation, we generally use 2 mg of Fe powder per sample which – converted to iron oxide and with the assumption that no significant precipitation of sample matrix occurs – will fit well into the Al sample holders that are used at the VERA AMS facility. As such, there exists a limiting ratio of sample volume to mass of Fe added (2 mg) above which the co-precipitation will no longer be quantitative.[5] For samples with volumes of $\leq$ 250 mL, addition of 2 mg of Fe will ensure a quantitative co-precipitation.[6]

For use of Actinide Resin, there exists a very similar limit for the sample volumes that can be prepared for multi-actinide analysis. After Actinide Resin is used to separate the actinide group from solution, the extractant of Actinide Resin has to be dissolved from the resin substrate with an alcohol (e.g. isopropanol).[3] In order to adapt and develop this procedure for AMS analysis, we have introduced the following steps: addition of Fe solution with an appropriate amount of Fe (equivalent to 2 mg) to the isopropanol solution; evaporation of the resulting solution in a crucible; conversion to the final target material by oxidation to iron oxide in an oven. As we previously tested, without addition of Fe to the isopropanol-extractant solution, a thin white layer of extractant ash would form in the crucible after conversion in the oven that cannot be mechanically recovered. In the developed procedure, the amount of Fe added will be the limiting factor for the final mass of the target material (thus, we added Fe solution equivalent to 2 mg of Fe). We have found, by testing, that 8 mg of Actinide Resin and 2 mg of Fe convert to a homogeneous residue that can be scraped out of the crucible. However, when testing for 20 mg of Actinide Resin and 2 mg of Fe, a thin white layer is visible in the crucible together with the residue, indicating that not all of the extractant has bound to the Fe oxide and can be recovered. In this way, we have found that this ratio of Actinide Resin to added Fe is appropriate for the described sample systems and is what we currently recommend. Finally, the amount of Actinide Resin (8 mg) used will limit the sample volume that can be optimally processed. Horwitz et al. found that the extraction is quantitative up to a limit of 250 mg of resin per L of sample,[3] i.e. a maximum of 32 mL of (evaporated) sample solution for use of 8 mg of resin.

For all experiments that we performed with this method, we used quartz glass crucibles for ashing of the resin extractant, because they work well for $Fe(OH)_3$ co-precipitation and were available. However, because of the diphosphonic acid functional group of the DIPEX® extractant of Actinide Resin, decomposition of the extractant when ashing will release phosphoric acid, which will attack the quartz material and lead to visible etching after only one use of the crucible. While we could not detect any cross-contamination for a blank sample we prepared with a previously used crucible, and cleaning of the crucibles seemed to work well when boiling in HCl, continuous use of the same crucibles will likely complicate the cleaning process and lead to increased risk of cross-contamination. The use of a metal crucible that is resistant to phosphoric acid seems preferable.

Furthermore, we recommend the use of crucibles of a sufficient size for the ashing process. After drying the isopropanol-extractant-iron mixture in a plastic sample vial, we used a few drops of isopropanol to transfer the sticky, oily extractant residue to the crucible, where it was left to dry, once again. Notably, the evaporation of the isopropanol will push the oily residue up the wall of the respective container and even out of the crucible if the walls are not high enough. We ended up using 5 mL crucibles that turned out too big, but still, the residue crept up to ca. half-height of the walls. Using crucibles of appropriate size may also reduce the time needed to scrape the final sample specimen out of the crucible after ashing.

It should also be noted that the final sample material could not be recovered quantitatively from the crucible. A fraction of the material will stick to the wall and will be effectively lost. To a certain extent, the recovery of sample material will depend on the size of the crucible and the thoroughness of the experimenter when scraping the material from the crucible.

References

[1] P. Povinec, C. Badie and A. Baeza, *Journal of Radioanalytical and Nuclear Chemistry*, 2002, **251**, 369–374.

[2] M. K. Pham, M. Betti, P. P. Povinec, M. Benmansour, V. Bünger, J. Drefvelin, C. Engeler, J. M. Flemal, C. Gascó, J. Guillevic, R. Gurriaran, M. Groening, J. D. Happel, J. Herrmann, S. Klemola, M. Kloster, G. Kanisch, K. Leonard, S. Long, S. Nielsen, J.-S. Oh, P. U. Rieth, I. Östergren, H. Pettersson, N. Pinhao, L. Pujol, K. Sato, J. Schikowski, Z. Varga, V. P. Vartti and J. Zheng, *Journal of Radioanalytical and Nuclear Chemistry*, 2011, **288**, 603–611.

[3] E. Horwitz, R. Chiarizia and M. L. Dietz, *Reactive and Functional Polymers*, 1997, **33**, 25–36.

[4] B. Lafuente, R. T. Downs, H. Yang and N. Stone, *Highlights in Mineralogical Crystallography*, De Gruyter (O), 2015, pp. 1–30.

[5] F. Quinto, R. Golser, M. Lagos, M. Plaschke, T. Schäfer, P. Steier and H. Geckeis, *Analytical Chemistry*, 2015, **87**, 5766–5773.

[6] J. Qiao, X. Hou, P. Steier and R. Golser, *Analytical Chemistry*, 2013, **85**, 11026–11033.